

# A multi-scale simulation study for optimization and variability evaluation of molecular based flash cell

Vihar P. Georgiev *Member, IEEE*, Laia Vilà-Nadal, Leroy Cronin and Asen Asenov, *Fellow, IEEE*

**Abstract**— This paper presents computational simulation of a conceptual low power non-volatile memory cell based on inorganic molecular metal oxide clusters (*polyoxometalates* (POM)). The storage media is embedded in the gate dielectric of a Fully Depleted Silicon On Insulator (FDSOI) device. The simulations are carried out using a multi-physics simulation framework, which allows us to evaluate the variability in the programming window of the molecular based flash cell with an 18 nm gate length. We have focused our study on the threshold voltage variability influenced by random dopant fluctuations and random special fluctuations of the molecules in the floating gate of the flash-cell. Our simulation framework and conclusions can be applied not only to the POM-based flash cell but also to flash cells based on alternative molecules used as a storage media.

## I. INTRODUCTION

The field of molecular electronics continues to spur interest in the quest for miniaturization and reduction of operational power of electron devices. Most of the systems described in the literature are based on organic molecules, such as benzene, ferrocene and fullerenes [1]. However, the use of inorganic molecules known as polyoxometalates (POMs) (see Fig.1 and Fig.2) could offer several important advantages over the conventional and organic based devices. Our present work shows that the POMs are more compatible with existing CMOS processes than organic molecules and they can replace the polysilicon floating gate in contemporary flash cell devices [2-5]. The interest in POMs for flash cell applications stems from the fact that POMs are highly redox active molecules and that they can also be doped with electronically active heteroatoms [6]. They can undergo multiple reversible reductions/oxidations, which makes them attractive candidates for multi-bit storage in flash memory cells. The molecular charge storage is localised, thus minimising cross-cell capacitive coupling, which arises from charge redistribution on the sides of a poly-Si floating gate (FG) and is one of the most critical issues with flash memories. Although this benefit is presently realised in floating gates by charge-trapping dielectric or by a metallic nano-cluster array, both technologies exhibit large variability. Charge-trap memories suffer variation in trap-density and trap energy and the size and density of nano-clusters is difficult to control. This precludes their ultimate miniaturization. In fact, the concept of using molecules as storage centers has already been demonstrated for organic redox-active molecules [1].

In our previous work, we already introduced the concept of a POM based BULK and FDSOI flash cell [3]. We established that due to high doping concentration in the channel, the BULK cell shows higher variability in comparison to the FDSOI [4]. Also the FDSOI architecture provides excellent

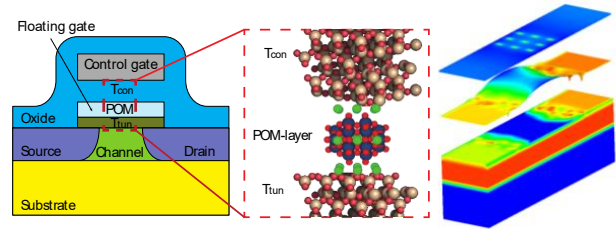


Fig. 1 Left - Schematic representation of a single-transistor FDSOI non-volatile memory cell, indicating the aimed substitution of the poly-Si floating gate (FG) with an array of polyoxometalate clusters (POM layer). The green balls are point charges representing the cations, which surround each POM in the experiment. Right - 3D electrostatic potential in oxide and the substrate. Fingerprint of the 3x3 POMs in the gate and the random dopant in the source and the drain are clearly visible.

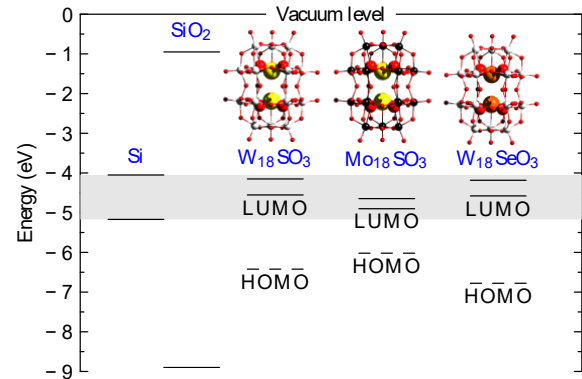


Fig. 2 Energy diagram comparing the conduction and valence band edges of Si and SiO<sub>2</sub> relative to the HOMO and LUMO levels of three POMs. Ball-and-stick view (insert) of three non-classic Wells-Dawson structure W<sub>18</sub>SO<sub>3</sub> - [W<sub>18</sub>O<sub>54</sub>(SO<sub>3</sub>)<sub>2</sub>]<sup>4+</sup>; M<sub>18</sub>SO<sub>3</sub> - [M<sub>18</sub>O<sub>54</sub>(SO<sub>3</sub>)<sub>2</sub>]<sup>4+</sup> and W<sub>18</sub>SeO<sub>3</sub> - [W<sub>18</sub>O<sub>54</sub>(SeO<sub>3</sub>)<sub>2</sub>]<sup>4+</sup>.

electrostatic integrity, due to low channel doping, leading to low native statistical variability. This is important for low power applications, which is the main requirement for the contemporary device technology.

Here, using full 3D simulations, we evaluate correlation between the device performance (in terms of threshold voltage  $V_T$ ) and statistical variability, arising from the random dopant fluctuations (RDF) and POM fluctuations (POMF). We also investigate dependence of the threshold voltage on the gate material and the oxide thickness.

## II. SIMULATION METHODOLOGY

In order to evaluate the performance of POMs as storage centers in the floating gate (FG) in the flash cell memories, we develop a simulation flow [7] [8], that links density functional theory (DFT) to the commercial three-dimensional (3D)

Research is supported by UK EPSRC platform grant EP/H024107/1.

Vihar P. Georgiev and Asen Asenov are with Device Modelling Group, School of Engineering, University of Glasgow, G12 8LT, Glasgow, UK.

Laia Vilà-Nadal and Leroy Cronin are with WestCHEM, School of Chemistry, University of Glasgow, G12 8QQ, Glasgow, UK.

Corresponding author: Vihar.Georgiev@glasgow.ac.uk

numerical simulator GARAND. Key component of this flow is the custom-built *Simulation Domain Bridge*, connecting the two distinct simulation domains – DFT for the molecular part and continuous device modeling section for the device modeling part. The main motivation for using this variety of computational techniques is the complexity of the problem. On the one hand, accurate description of the POM clusters requires first principles calculations, which in this work are based on the DFT method. On the other hand, descriptions of the current flow through devices demand the mesoscopic device approach provided by the TCAD software. Once the charge for the POM is obtained from the DFT program and it is transferred to the 3D numerical TCAD simulator, a drift-diffusion transport formalism is applied. It includes quantum corrections by means of the density-gradient approach.

### III. FLASH CELL DESIGN

The key design parameters of our template flash memory cell are based on our recent publication [9]. For the purpose of this study, an n-channel FDSOI flash memory cell with an 18 nm square gate has been designed (Fig.1). It is based on a previously studied 18 nm ‘template’ transistor and it is similar to the contemporary flash cells studied elsewhere [10].

Given that the gate area of the template flash cell is 18 x 18 nm<sup>2</sup>, we consider sheet densities  $N_S$  of POM clusters, approximately  $2.8 \times 10^{12}$  cm<sup>-2</sup> corresponding to nine metal clusters arranged in a 3x3 rectangular planar grid. The control oxide thickness  $T_{con}$  (see Fig.1) is 15.6 nm. The tunneling oxide thickness  $T_{tun}$  consists of a 3 nm high-quality SiO<sub>2</sub>. The [W<sub>18</sub>O<sub>54</sub>(SeO<sub>3</sub>)<sub>2</sub>]<sup>4+</sup> POM layer thickness is 3 nm, including the balancing cations, (C<sub>4</sub>H<sub>9</sub>)<sub>4</sub>N<sup>+</sup> (tetra-butyl ammonium (TBA)). The molecule itself is negatively charged and, in order to keep the entire system neutral, in the experiment each POM is surrounded by positively charged molecules – cations (green balls in Fig.1). Together they form an insulating barrier of permittivity close to that of SiO<sub>2</sub> [11]. The POMs are oriented parallel to the SiO<sub>2</sub> surfaces. All simulations are performed at low drain bias ( $V_{DS} = 50$  mV).

Fig.2 shows a key result of the DFT calculations for three POM clusters. The energy levels of the highest occupied and lowest unoccupied molecular orbitals (HOMO and LUMO, respectively) for all molecules are favourably aligned below the conduction band of Si and they could be effectively insulated by a comparatively high potential barrier of SiO<sub>2</sub>. From this point of view all three molecules are similar, however only the W<sub>18</sub>SeO<sub>3</sub> - [W<sub>18</sub>O<sub>54</sub>(SeO<sub>3</sub>)<sub>2</sub>]<sup>4+</sup> cluster shows numerous oxidation and reduction properties [2]. That gives more possibilities to design a practical molecular based flash cell. As a result, in this work we concentrate our discussions on this specific molecule – W<sub>18</sub>SeO<sub>3</sub>.

Also, as a further step in our flash cell design, we consider correlation between different thicknesses of the tunneling gate oxides ( $T_{tun}$ ) and difference of the threshold voltage ( $\Delta V_T$ ) (Fig.3). Moreover, we introduce a high-K gate material – Al<sub>2</sub>O<sub>3</sub>. Fig.3 reveals that flash cells with SiO<sub>2</sub> as a gate material have wider programming windows ( $\Delta V_T$ ) in comparison to devices with Al<sub>2</sub>O<sub>3</sub> as a FG. Also, for both gate materials the programming window has the highest value at  $T_{tun}=1.5$  nm. Hence, the best option is to design a flash cell where the tunneling oxide is 1.5 nm and the gate material is SiO<sub>2</sub>. However, a flash cell with 1.5nm SiO<sub>2</sub> might have poor retention characteristics. For this reason, here we study a flash

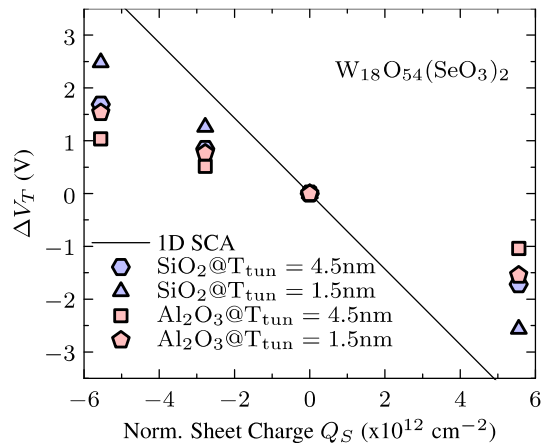


Fig. 3 Comparison between sheet charge approximation (SCA) and the numerical results of the simulated flash cell for two gate materials (SiO<sub>2</sub> & Al<sub>2</sub>O<sub>3</sub>) at two  $T_{tun}$  oxide values (4.5 nm & 1.5 nm).

cell with  $T_{tun}=4.5$  nm and SiO<sub>2</sub> as a gate material. Also, such flash cell design is consistent with our previous work, which will allow us to draw coherent conclusions [9].

### IV. STATISTICAL VARIABILITY

#### A. Constraint number of nine POMs in the oxide

In order to obtain realistic results for threshold voltage variability in the FDSOI flash cell with POM molecules as a storage media, we introduce three sets of 1,000 devices. Each set has two sources of statistical variability, such as random dopant fluctuations (RDF) and POMs fluctuations (POMF). We incorporate the charge density of nine [W<sub>18</sub>O<sub>54</sub>(SeO<sub>3</sub>)<sub>2</sub>]<sup>4+</sup> POMs (shown in Fig.1) as a charge storage center. It should be emphasised that for all three sets of 1,000 devices composing the ensembles, the number of POMs is constant and it equals nine. In the case of the RDF only calculations, the charge storage clusters are arranged in a regular grid of 3x3 POMs centered within the gate (right hand side of Fig.1). In the POMF only calculations, the molecules are randomly displaced laterally in relation to the regular 3x3 grid used previously. Finally, in the third case, both of these variations, i.e., RDF and POMF, are included.

Four distinct  $V_T$  values related to the four easily accessible oxidation/redox states of the molecular cluster can be obtained. They are presented in Table I as follows: parent (neutral) POMs have no charge in the clusters. In 1x red. state, each POM has one electron more in comparison to the parent molecule. Hence, the total number of charges in the floating gate is equal to -9q (q-charge of an electron). In 2x red. state, each POM has two electrons more in comparison to the parent cluster, corresponding to the total number of -18q charges in the floating gate. In 2x ox. state, each POM has two electrons less in comparison to the parent cluster, corresponding to the total number of +18q charges in the floating gate.

Table I presents the statistics of an average value ( $\mu$ ) and the standard deviation ( $\sigma$ ) of four different  $V_T$  values for three different cases: devices with only random dopants present (RDF only), transistors with only POMs fluctuation present (POMF only) and cells with combined RDF and POMF (RDF+POMF). All results are compared to the nominal values of the flash cell with continuous doping.

Fig.4, Fig.5 and Fig.6 present the same data as Table I but in a graphical form. Each figure shows the probability density

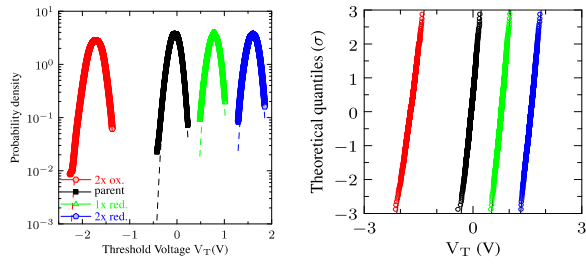


Fig. 4 Left: Probability density function (PDF); Right: normal probability plot of the same distribution function of the  $V_T$  distribution for each bit of 1,000 devices with *RDF only*. Dashed line is a Gaussian fit.

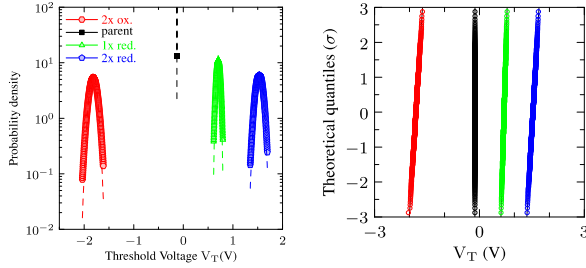


Fig. 5 Left: Probability density function (PDF); Right: normal probability plot of the same distribution function of the  $V_T$  distribution for each bit of 1,000 devices with *POMF only*.

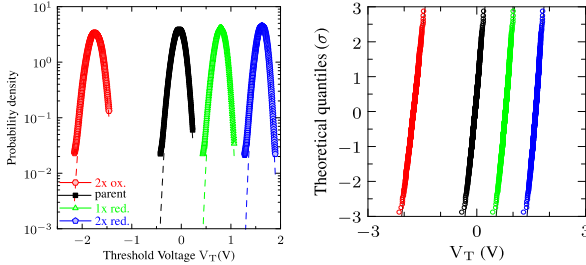


Fig. 6 Probability density function (PDF); Right: normal probability plot of the same distribution function of the  $V_T$  distribution for each bit of 1,000 devices with combined variability (*RDF with POMF*).

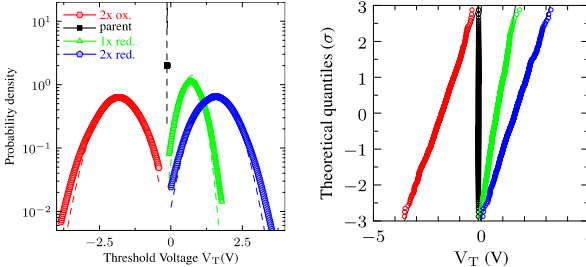


Fig. 7 Probability density function (PDF); Right: normal probability plot of the same distribution function of the  $V_T$  distribution for each bit of 1,000 devices without *RDF* and with *Poisson POMF*.

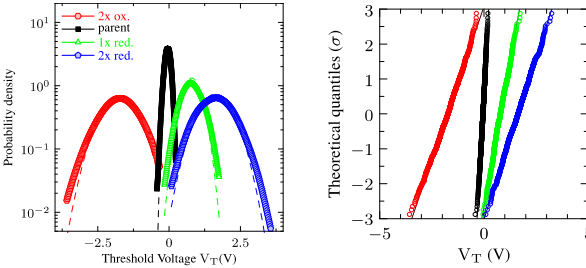


Fig. 8 Probability density function (PDF); Right: normal probability plot of the same distribution function of the  $V_T$  distribution for each bit of 1,000 devices with *RDF and Poisson POMF*.

function (PDF) and standard deviation ( $\sigma$ ) for an ensemble of

TABLE I. NOMINAL THRESHOLD VOLTAGE OF THE FDSOI CELL, ENCODING 4 BITS FOR CONTINUOUS FLASH; CORRESPONDING AVERAGE AND STANDARD DEVIATION VALUES FOR THE THREE ENSEMBLES WITH VARIABILITY.

Bit (Hex) redox state	Nominal $V_T$	RDF 1000 devices		POMF 1000 devices		RDF+POMF 1000 devices	
	$V_T$ (V)	$V_T$ (V)	$\sigma V_T$ (mV)	$V_T$ (V)	$\sigma V_T$ (mV)	$V_T$ (V)	$\sigma V_T$ (mV)
2x ox.	1.952	-1.726	125	-1.817	63	-1.747	107
parent	-0.056	-0.051	92	-0.129	0	-0.052	92
1x red.	0.902	0.775	88	0.703	29	0.786	84
2x red.	1.743	1.594	94	1.529	58	1.610	105

TABLE II. NOMINAL THRESHOLD VOLTAGE OF THE FDSOI CELL, ENCODING 4 BITS FOR CONTINUOUS FLASH. POISSON DISTRIBUTION OF THE POMs IS CONSIDERED. CORRESPONDING AVERAGE AND STANDARD DEVIATION VALUES FOR THE THREE ENSEMBLES WITH VARIABILITY.

Bit (Hex) redox state	Nominal $V_T$	POMF 1000 devices		RDF+POMF 1000 devices	
	$V_T$ (V)	$V_T$ (V)	$\sigma V_T$ (mV)	$V_T$ (V)	$\sigma V_T$ (mV)
2x ox.	1.952	-1.848	568	-1.754	596
parent	-0.056	-0.129	0	-0.052	92
1x red.	0.902	0.723	287	0.793	301
2x red.	1.743	1.565	541	1.628	541

1,000 devices with RDF only, POMF only and RDF + POMF, correspondingly. Based on our numerical calculations displayed above, we can draw the following important conclusions.

Firstly, the curves presenting the PDF for all devices with RDF (Fig.4 and Fig.6) are broader in comparison to the POMFs only case (Fig.5). This is reflected in the values of the standard deviation shown in Table I where all flash cells with RDF+POMF have standard deviation of around 100 mV, while in the case of the POMF only calculations this value varies from 0 to 63 mV. Hence, it can be concluded that the RDF has stronger impact on the  $\sigma V_T$  in comparison to the POMF only scenario. Additionally, the two sources of variability show similar behaviour and the main foundation of variability is indeed the RDF. Also, in all calculations the results fit well with the Gaussian distribution (dashed line in Fig.4 – Fig.6).

Secondly, for the FDSOI continuous doping structures the average value of  $V_T$  for each bit has higher values in comparison to the average values of  $V_T$  for the RDF only, POMF and RDF+POMF cells. Also, the standard deviation increases in the RDF cells with increasing of the redox state of the molecule and  $\sigma$  increases with the increase of the negative charge in the POM. However, this reflects a known dependence of variance on the number of charges in the oxide [12]. This dependence is much stronger and it is reflected in the RDF+POMF ensemble too.

Thirdly, in the case of the continuous doped FDSOI device the average value of  $V_T$ , needed for the cell to change the oxidation state by one electron for each POM is 0.96 V and 0.84 V. In the case of the RDF, POMF RDF+POMF structures the  $V_T$  steps are almost identical and they are around 0.74 V and 0.83V for the first and the second step of oxidation, respectively. Hence, there appears to be an almost negligible degradation of the average programming window with sources of statistical variability in comparison to the continuous cells.

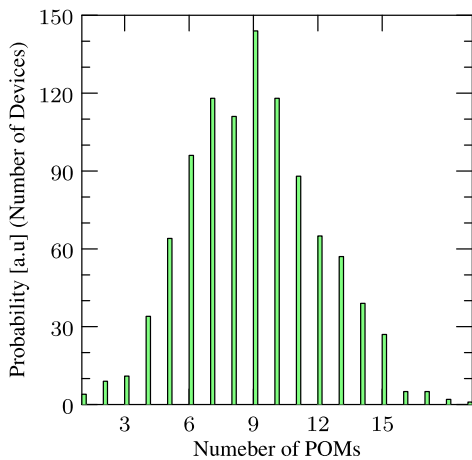


Fig. 9 Histogram of the number of POMs for ensembles with POMF used in the Poisson distribution case.

Last but not least, it is clear from Fig.4 – Fig.6 that different bits do not overlap for this sample of 1,000 devices. Indeed, this is good news because it reveals the potential of realising the practical multi-bit flash cell. However, the bits are close to each other, specifically the parent bit and the two redox states. One possibility to overcome this problem is to use only two bits, e.g. 2x ox. and 2x red. They are separated by almost 3V and if we can control the exact number of POMs in the oxide this looks as a promising option. However, in the current molecular based technology this process is not well developed and in many cases the molecular layer is not uniformly distributed. For this reason, in the next section we investigate the dependence of the voltage threshold on the number of POMs in the FG that follows the Poisson distribution.

#### B. Poisson distribution of POMs in the oxide

Fig.7, Fig.8 and Table II present data for devices where the Poisson distribution in the POMs in the FG is considered. The actual Poisson distribution is presented in Fig.9 and it is identical for all devices. As shown in Fig.9, it is possible to have cells with as few as 1 molecule and as many as 19 POMs. Comparing the data from the previous and this section, the following conclusions can be established.

Firstly, as expected, the standard deviation is up to 5 times higher in comparison to the standard deviation for only 9 POMs in the FG. However, average value ( $\mu$ ) is similar in both cases. Secondly, results fit well with the Gaussian distribution (dashed line in Fig.7 and Fig.8) except for the tails of the curves. Such discrepancy between analytical approximations and numerical calculations emphasizes the importance of numerical simulation in determining performance of the devices.

More importantly the four bits start to overlap significantly. This is similar to the data reported for the BULK case [3]. Hence, in this case the advance of the FDSOI flash cell design is not visible anymore. As a result, we need to ensure that in the fabrication process a uniform distribution of the POMs film in the oxide is achievable in order to realize the practical molecular based flash cell.

## V. CONCLUSION

In this work, we compare the statistical threshold voltage variability of the molecular based 18-nm FDSOI flash cells.

Two sources of statistical variability, RDF and POMF, are discussed. Also, we establish that the RDF variability is the dominant factor, which influences the  $V_T$  distribution. Our work shows that the Poisson distribution of POMs in the FG could diminish the benefit of the FDSOI architecture in comparison to the BULK device. Moreover, our approach provides both qualitative and quantitative insight toward the design and optimisation of such molecular-based flash cell, particularly in the context of sources of statistical variability. Most importantly, we show that controlling the number of POMs in the oxide is critical in order to achieve the optimal device performance. In the future work, we will concentrate our efforts to close the circle between creating physical devices and designing fabrication process in order to create reliable, low power molecular base flash cell.

## REFERENCES

- [1] H. Zhu and Q. Li, "Novel Molecular Non-Volatile Memory: Application of Redox-Active Molecules," *Applied Sciences*, vol. 6, p. 7, 2015.
- [2] C. Busche, L. Vila-Nadal, J. Yan, H. N. Miras, D. L. Long, V. P. Georgiev, *et al.*, "Design and fabrication of memory devices based on nanoscale polyoxometalate clusters," *Nature*, vol. 515, pp. 545-549, Nov 27 2014.
- [3] V. P. Georgiev, S. M. Amoroso, T. M. Ali, L. Vila-Nadal, C. Busche, L. Cronin, *et al.*, "Comparison Between Bulk and FDSOI POM Flash Cell: A Multiscale Simulation Study," *IEEE Transactions on Electron Devices*, vol. 62, pp. 680-684, Feb 2015.
- [4] V. P. Georgiev, S. M. Amoroso, L. Vila-Nadal, C. Busche, L. Cronin, and A. Asenov, "FDSOI molecular flash cell with reduced variability for low power flash applications," *Proceedings of the 2014 44th European Solid-State Device Research Conference (Essderc 2014)*, pp. 353-356, 2014.
- [5] V. P. Georgiev, S. Markov, L. Vila-Nadal, C. Busche, L. Cronin, and A. Asenov, "Multi-scale computational framework for the evaluation of variability in the programming window of a flash cell with molecular storage," *2013 Proceedings of the European Solid-State Device Research Conference (Essderc)*, pp. 230-233, 2013.
- [6] D. L. Long, R. Tsunashima, and L. Cronin, "Polyoxometalates: building blocks for functional nanoscale systems," *Angew Chem Int Ed Engl*, vol. 49, pp. 1736-58, Mar 1 2010.
- [7] V. P. Georgiev and A. Asenov, "Multi-scale Computational Framework for Evaluating the Performance of Molecular Based Flash Cells," in *Numerical Methods and Applications: 8th International Conference, NMA 2014, Borovets, Bulgaria, August 20-24, 2014, Revised Selected Papers*, I. Dimov, S. Fidanova, and I. Lirkov, Eds., ed Cham: Springer International Publishing, 2015, pp. 196-203.
- [8] L. Vila-Nadal, S. G. Mitchell, S. Markov, C. Busche, V. Georgiev, A. Asenov, *et al.*, "Towards Polyoxometalate-Cluster-Based Nano-Electronics," *Chemistry – A European Journal*, vol. 19, pp. 16502-16511, 2013.
- [9] V. P. Georgiev, S. Markov, L. Vila-Nadal, C. Busche, L. Cronin, and A. Asenov, "Optimization and Evaluation of Variability in the Programming Window of a Flash Cell With Molecular Metal-Oxide Storage," *IEEE Transactions on Electron Devices*, vol. 61, pp. 2019-2026, Jun 2014.
- [10] A. Maconi, S. M. Amoroso, C. M. Compagnoni, A. Mauri, A. S. Spinelli, and A. L. Lacaita, "Three-Dimensional Simulation of Charge-Trap Memory Programming &#x2014; Part II: Variability," *IEEE Transactions on Electron Devices*, vol. 58, pp. 1872-1878, 2011.
- [11] N. Glezos, P. Argitis, D. Velessiotis, and C. D. Diakoumakos, "Tunneling transport in polyoxometalate based composite materials," *Applied Physics Letters*, vol. 83, p. 488, 2003.
- [12] S. Markov, S. M. Amoroso, L. Gerrer, F. Adamu-Lema, and A. Asenov, "Statistical Interactions of Multiple Oxide Traps Under BTI Stress of Nanoscale MOSFETs," *IEEE Electron Device Letters*, vol. 34, pp. 686-688, 2013.